

# Ongoing meteor work

## Long-term variability of visual sporadic meteor rates

*Audrius Dubietis*<sup>1</sup> and *Rainer Arlt*<sup>2</sup>

Long-term variability of visual sporadic meteor rates is analyzed using Visual Meteor Data Base records collected in the years 1982–2007. It is found that sporadic meteor rates in the selected period of September vary within  $\pm 20\%$  around the average hourly rate of  $HR_{\text{spo}} = 11.7$ . These variations have a period of  $10.2 \pm 1.2$  years and exhibit a high degree of correlation (36%) with solar activity as expressed by the Zurich sunspot numbers. The occurrences of highest visual sporadic rates almost perfectly coincide with the sunspot maxima of 1990 and 2000. They support recent findings by Šimek and Pecina (2002) on a long-term radar sporadic meteor variability with the course of the solar cycle.

Received 2007 December 10

### 1 Introduction

The impact of solar variability on the terrestrial environment is apparent through numerous connections between the Sun and Earth, including the variability of space weather, stratospheric ozone production rates and climate (Lean 1997, Lean 2005). The most severe disturbances of the terrestrial environment are traced in the high atmosphere (ionosphere), where temperature and number density of charged particles at 150–800 km height varies within broad margins during the course of 11-year solar cycle. Specifically, auroras that typically emerge at 100–500 km height are the direct signatures of enhanced solar activity. Solar flares and coronal mass ejections resulting in solar wind gusts cause a rapid expansion of the auroral oval and extend auroral visibility down to mid-latitudes. The impact of solar variability on the mesosphere is manifested in a different manner, controlling the frequency of the occurrence of noctilucent clouds (Gadsden 1998, Romejko et al., 2003), and more generally, the periodic shrinking and expansion of the entire polar mesospheric cloud layer (DeLand et al., 2006). Unlike auroras, noctilucent clouds exhibit the lowest occurrence frequency at maximum solar activity, the ice crystal growth dynamics being related to solar radiation-induced changes in the ambient temperature and water vapor concentration at the mesopause level. Since meteoroid ablation heights straddle the border between the ionosphere and mesosphere, it is quite natural to expect that solar activity should have some detectable impact on the observed meteor rates as well.

Sir J.F. Herschel was probably the first who conjectured the link between meteor activity and the solar cycle. However, his idea was based on erroneous assumptions that the Sun gains its energy by converting kinetic energy of infalling meteoritic objects, and the sunspots are the scars left by those impacts (Hughes 1995). The problem of a possible link between the meteor rate variability and the solar cycle in its modern

formulation has been put forward some 80 years later by Bumba (1949), who studied meteor and fireball activity in the years 1844–1943 and concluded that highest meteor rates occur in the years close to the minimum of solar activity. The interest in possible solar influence on meteor rates has been brought back to attention after the anomalous increase of radar meteor counts reported worldwide in 1963. Hughes (1974) and Lindblad (1976) analyzed available records at that time and concluded that the frequency of radar meteor echoes varies inversely with the solar activity. Moreover, the magnitude of this variation was found to be considerable, suggesting an almost twofold increase of radar echoes close to the sunspot minimum (Lindblad, 2003). Lindblad (1978) and later Prikryl (1983) also established the idea that the geomagnetic activity influences the detected radar meteor rates on much shorter time scale (on the order of days) as well, with an apparent decrease of meteor echoes during geomagnetic storms. These analyses, however, did not strictly distinguish between the sporadic and shower meteors; the numbers of latter are strongly influenced by the local encounter conditions. The topic, however, still remains controversial since the most recent analysis of sporadic radar meteor rates, which covered more than a 40-year period (almost four solar cycles) arrived at the directly opposite result, indicating a strong (70%) correlation between the two processes of interest (Šimek and Pecina, 2002), with enhanced of radar sporadic meteor rates two years after the solar maximum.

### 2 Physical origins of meteor rate variability

The 11-year solar variability is barely detectable in the visible part of its spectrum. However, changes in the radiation flux are considerable in the radio wave, X-ray and in the extreme ultraviolet (EUV) spectral (100–250 nm) range. Enhanced EUV radiation is absorbed in the upper atmosphere, and therefore promotes enhanced ionization rates of the atmospheric gases. Energy excess raises the ambient temperature, the heating being relevant at 150–800 km height, with a temperature difference for the quiet and active Sun and as high as 500 K (Lean, 1997). A still appreciable change in

<sup>1</sup>Baltupio 101-2, LT-2040 Vilnius, Lithuania.  
Email: audrius.dubietis@ff.vu.lt

<sup>2</sup>Friedenstrasse 5, D-14109 Berlin, Germany.  
Email: rarlt@aip.de

ambient temperature of a few tens of degrees is traced down to 100 km, where meteoroid ablation processes are taking place.

Ellyett and Kennewell (1980) proposed a model of atmospheric density changes that qualitatively explained the variability of radar meteor rates as being due to atmospheric effects. According to their model, the terrestrial atmosphere experiences periodic compressions and expansions responding to changes in the flux of solar X-ray and EUV radiation. At low solar activity, meteoroids encounter a steeper atmospheric density gradient at ablation heights, which in turn results in ablation of a meteoroid of a given size over a shorter path length. Indeed, Lindblad (1976) measured that the endpoint heights of the radar-detected Perseid meteors vary considerably from 85 km near sunspot maximum to 96 km at sunspot minimum, thus indicating an apparent shortening of meteor trajectories at solar minimum. Interestingly, this is not the case for the beginning heights of meteoroid ablation, as was found by Porubčan and Getman (1992) from the height studies of photographic Perseid meteors. According to the model of Ellyett and Kennewell (1980), the detected meteor rates should be highly sensitive to their mass distribution index  $s$ . It is suggested that for  $s < 2$  a decrease of atmospheric density scale height results in an decrease of detected meteor rates, whereas for  $s > 2$  the trend is opposite. It is therefore expected that shower and sporadic meteor rates should behave differently during the course of the 11-year solar cycle. However, in the light of most recent results, new issues had been raised and plausible physical explanations seem to be missing. Pecina and Šimek (1999) analyzed long-term variations of the background sporadic radar meteor rates in December during the Geminid observing campaigns and derived a directly opposite relationship of radar sporadic rates to that of Lindblad, pointing to a high direct correlation between meteor rates and sunspot numbers. In an extended analysis, the same authors also obtained strong correlations for the January and August sporadic radar meteor rates (Šimek and Pecina, 2002). Their results point out that enhanced radar sporadic meteor rates are detected during the years of solar activity maximum, with a possible 1–2-year shift between the sunspot and radio-echo maxima as due to a secondary maximum of large solar flares, contrary to model predictions and previous observations.

On the other hand, it remains still an open question whether visual meteor rates respond to atmospheric density changes. In this respect, the only extended analysis of visual meteor rates performed so far is that of Bumba (1949). His assumptions, however, were based on relatively small meteor numbers collected by various observing techniques, and the topic deserves to be re-examined.

### 3 Data analysis

In order to study whether a relationship between the visual meteor rates and solar activity exists, our choice

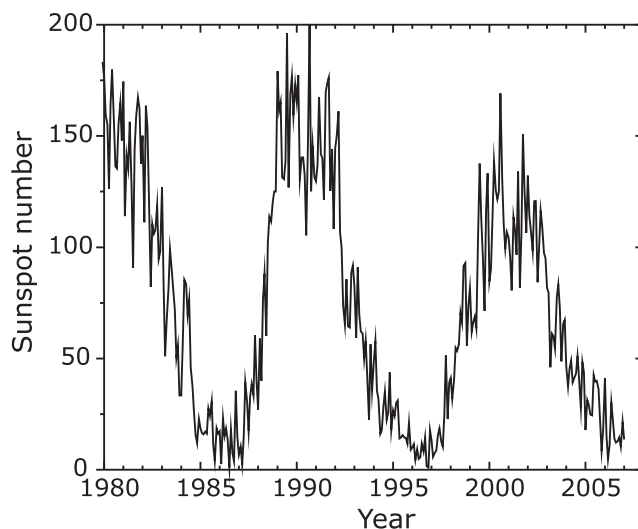


Figure 1 – Solar variability expressed by the monthly Zurich sunspot numbers from 1980 to 2007. (adapted from <http://solarscience.msfc.nasa.gov>.)

is cast on the sporadic meteor rates observed around the autumn equinox (September 10–30). Sporadic meteors represent a good target to be investigated, since their annual activity is well studied and is not affected by variable encounter conditions inherent to annual meteor showers. Sporadic meteors seem to emanate from rather randomly distributed radiant points. The only exception is a diffuse concentration of radiant points near the antihelion point. In September, the antihelion source is discriminated as a distinct meteor shower in the VMDB, formerly designated as (Southern) Piscids (SPI), and ANT in the modern meteor shower list; see (Arlt & Rendtel, 2006). In present analysis it has been subtracted from the dataset, in order to exclude apparent dependence of the sporadic meteor rates on the zenithal radiant distance. However, a weak dependence on the zenithal radiant distance (known as diurnal variation of the sporadic meteor numbers) still remains due to the extended apex source, which rises in the second half of the night. This factor has been minimized, since the bulk of observations were carried out during local evening hours. In order to avoid differences in sporadic rates seen from the northern and southern hemispheres, we also restricted ourselves to observations from the northern hemisphere where all the observing locations fit into an interval from  $30^\circ$  to  $60^\circ$  northern latitude. The chosen period of September 10–30 is free from any major shower activity; the available data on sporadic meteors contained in the Visual Meteor Database (VMDB) thus comprise a homogenous set of observations carried out by a standardized observing technique and amounts to a total of 29 369 sporadic meteors observed in the years from 1982 to 2007. The investigated period covers 26 years of observations, which equals to 2.5 solar cycles, whose variability is represented in terms of the Zurich sunspot numbers (also known as Wolf numbers) plotted in Fig. 1, using data from <http://solarscience.msfc.nasa.gov>.

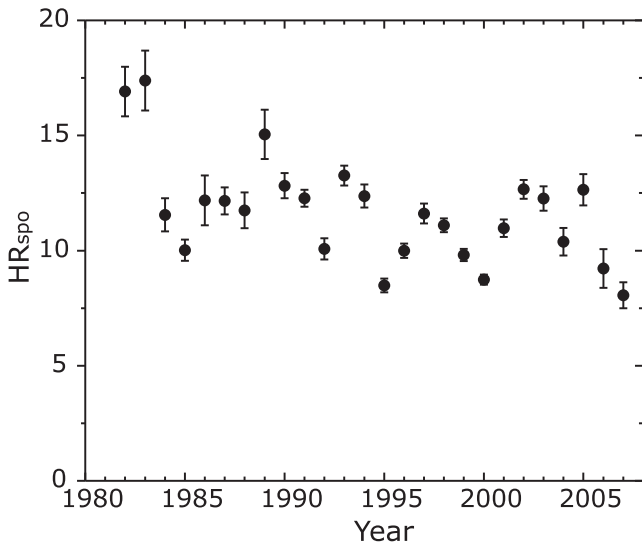


Figure 2 – Average sporadic meteor hourly rates of September derived for limiting magnitudes  $lm \geq 6.0$ .

The hourly rate for sporadic meteors,  $HR_{\text{spo}}$  was calculated using a standard procedure:

$$HR_{\text{spo}} = \frac{N_{\text{spo}} r^{6.5 - lm} F}{T_{\text{eff}}}, \quad (1)$$

where  $N_{\text{spo}}$  is the individual number of sporadic meteors observed during a time period  $T_{\text{eff}}$ ,  $lm$  is the limiting magnitude,  $r$  is the magnitude population index and  $F$  is the field obstruction factor. The error bars were estimated as:

$$\Delta HR_{\text{spo}} = \frac{HR_{\text{spo}}}{\sqrt{\sum_i N_{\text{spo}}}}. \quad (2)$$

In the analysis we applied a constant magnitude population index of  $r = 3.00$ , which was obtained using the evaluation procedure described in detail by Arlt (2003). For hourly rate calculations we have chosen only the observations with limiting magnitudes  $lm \geq 6.0$ , since the expected impact of solar activity (if any) might be pronounced on faint meteors only. A single average value of  $HR_{\text{spo}}$  was calculated for each year, and the long-term activity profile obtained is illustrated in Fig. 2. The numerical data of the sporadic meteors and the sunspot numbers are given in Table 1. The resulting long-term activity profile suggests that some variations of sporadic meteor hourly rates indeed are taking place, oscillating around the average value of  $HR_{\text{spo}} = 11.7$ . The mean amplitude of this oscillation is  $\pm 2.3$  and does not exceed  $\pm 20\%$ , however being still well-detectable above the error bars estimated for each individual data point.

A straightforward method to verify if any periodicity in time variations of a given process (sporadic meteor hourly rates) exists is to calculate its auto-correlation function, which means sampling the dataset with itself introducing a time shift. Statistically the autocorrela-

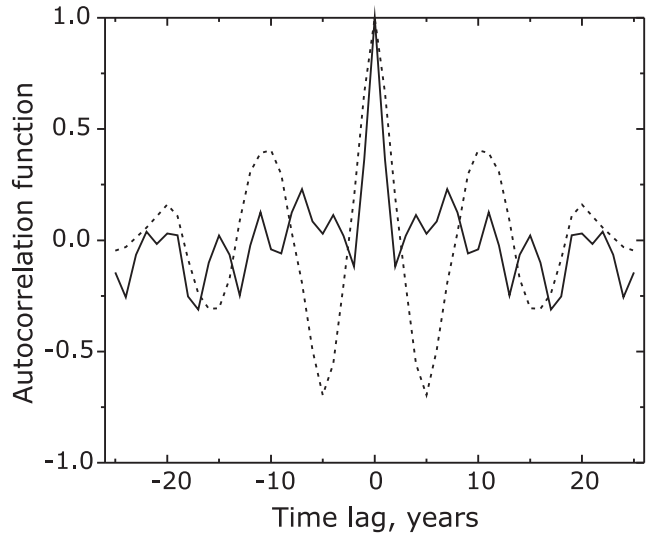


Figure 3 – Autocorrelation function of sporadic meteor hourly rates (solid curve) and sunspot numbers (dashed curve).

Table 1 – Numerical data of the visual sporadic meteor activity in the period of September 10–30, 1982–2007.  $N_{\text{spo}}$  is the total number of observed sporadic meteors,  $n_{\text{obs}}$  is the number of contributing observers,  $HR_{\text{spo}}$  is the average hourly rate calculated for limiting magnitudes  $lm \geq 6.0$ ,  $S_n$  is the Zurich sunspot number for September taken from <http://solarscience.msfc.nasa.gov>.

Year	$N_{\text{spo}}$	$n_{\text{obs}}$	$HR_{\text{spo}}$	$S_n$
1982	361	17	$16.9 \pm 1.1$	118.8
1983	452	12	$17.4 \pm 1.3$	50.3
1984	345	9	$11.6 \pm 0.7$	15.7
1985	1109	39	$10.0 \pm 0.5$	3.9
1986	575	22	$12.2 \pm 1.1$	3.8
1987	621	21	$12.2 \pm 0.6$	33.5
1988	346	18	$11.8 \pm 0.8$	120.1
1989	375	16	$15.1 \pm 1.1$	176.7
1990	727	18	$12.8 \pm 0.6$	125.2
1991	1441	32	$12.3 \pm 0.4$	125.3
1992	796	18	$10.1 \pm 0.5$	63.9
1993	1564	43	$13.3 \pm 0.4$	22.4
1994	896	28	$12.4 \pm 0.5$	25.7
1995	1127	30	$8.5 \pm 0.3$	11.8
1996	1862	39	$10.0 \pm 0.3$	1.6
1997	2432	42	$11.6 \pm 0.4$	51.3
1998	2688	60	$11.1 \pm 0.3$	92.9
1999	4015	67	$9.8 \pm 0.3$	71.4
2000	2365	35	$8.7 \pm 0.2$	109.9
2001	1075	23	$11.0 \pm 0.4$	150.7
2002	1115	17	$12.7 \pm 0.4$	109.5
2003	627	11	$12.3 \pm 0.5$	48.7
2004	397	12	$10.4 \pm 0.6$	27.7
2005	514	14	$12.6 \pm 0.7$	22.1
2006	1335	13	$9.2 \pm 0.8$	14.5
2007	209	2	$8.1 \pm 0.6$	6.2

tion function reads as:

$$ac(l) = \frac{(\overline{HR_{\text{spo}}(t) - \overline{HR_{\text{spo}}}})(\overline{HR_{\text{spo}}(t+l) - \overline{HR_{\text{spo}}}})}{\sigma(HR_{\text{spo}})}, \quad (3)$$

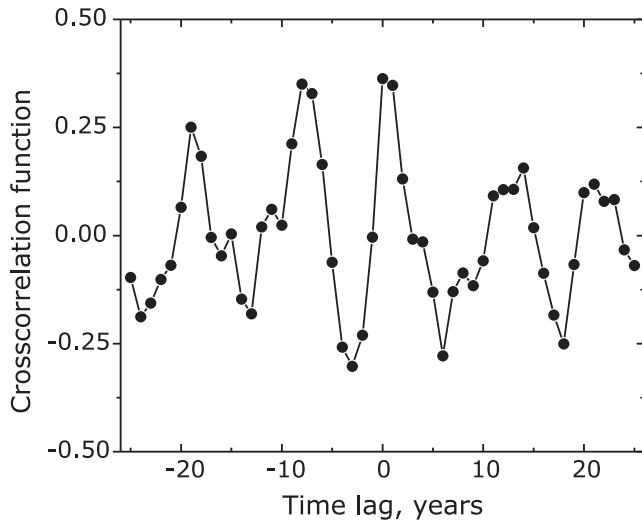


Figure 4 – Calculated cross-correlation function between  $HR_{\text{spo}}$  and  $S_n$ .

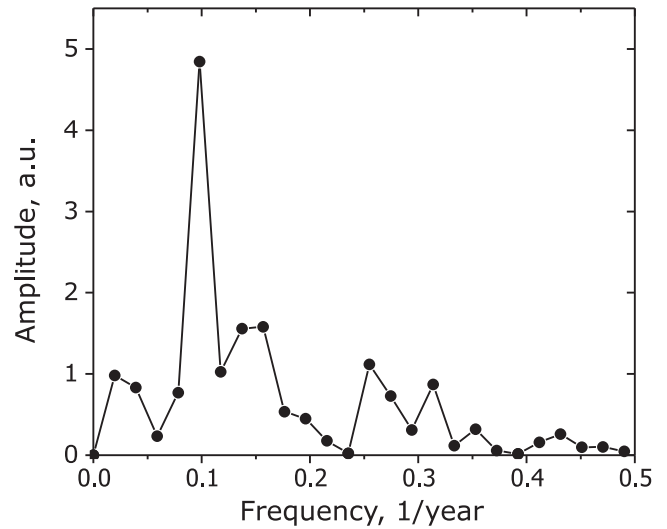


Figure 5 – Frequency spectrum of the cross-correlation function.

where where  $l$  denotes the time lag, the overline operator means time averages, and  $\sigma(HR_{\text{spo}})$  is the variance of the time series of sporadic meteor hourly rates.

Obviously, the auto-correlation function is symmetric and yields perfect unity at zero time delay (time lag). It is also worth mentioning that fewer data points contribute to the auto-correlation function at large time lag, with the leftmost and the rightmost points in the  $ac(l)$  plot being produced just by two single marginal points from the hourly rate dataset. The result is plotted in Fig. 3. The auto-correlation data (solid curve) shows that weak, but still clearly detectable periodic variations in sporadic meteor hourly rates are present over a  $\sim 10$ -year time scale. The effect of periodicity is visually amplified by adding an auto-correlation function of the sunspot numbers depicted by a dashed curve. It has to be noted that more data would notably improve the precision of our calculations, which crucially depends on the ratio between the expected (11-year) variability period and the actual time scale covered by the observations (26 years). Since the individual auto-correlation functions for each process are always symmetric, it provides almost no information how in fact the two processes are coupled together. Therefore we take a second step in the statistical analysis, which involves the calculation of the cross-correlation function:

$$cc(l) = \frac{(HR_{\text{spo}}(t) - \overline{HR_{\text{spo}}})(S_n(t+l) - \overline{S_n})}{\sqrt{\sigma(HR_{\text{spo}})\sigma(S_n)}}, \quad (4)$$

where the meanings and notations of physical quantities are the same as in Eqn. 3. Differently from the auto-correlation, the sampling between the two time-shifted variables (sporadic meteor hourly rates and sunspot numbers) is performed here. The values of  $cc(l)$  always fall into the range between  $-1$  (inverse correlation) and  $1$  (direct correlation), while  $0$  corresponds to no correlation at all. It is important to note that the cross-correlation function reveals not only the strength of a mutual coupling, but also the phase shift between the two processes varying in time. The calculated cross-

correlation function  $cc(l)$  is plotted in Fig. 4. It suggests a high degree of correlation between the two variables with the highest value of  $cc(l) = 0.36$  and distinct periodic oscillations on an approximately 10-year time scale. It is interesting to note that we obtained a lower cross-correlation coefficient by choosing a lower limit for  $lm$  for the data selection (function not shown). Another relevant feature seen from the plot is that the positive cross-correlation peak nearly coincides with a 0 time lag, indicating that maximum sporadic rates occur shortly (within one year) after the sunspot maximum. The results obtained are almost identical to those reported by Pecina and Šimek (1999) and Šimek and Pecina (2002), who found a similar relationship and a similar phase shift of radar sporadic meteor rates with respect to sunspot numbers.

Finally, we have evaluated more precisely the oscillation period by performing a frequency analysis by means of a Fourier transform on the  $cc(l)$  data. The Fourier frequency spectrum is depicted in Fig. 5. It indicates a prominent peak at  $1/T = 0.098 \text{ yr}^{-1}$ , suggesting a variability period of  $T = 10.2 \pm 1.2$  years, the error bars being evaluated from the estimation of the full width at half maximum of the peak. For a given time resolution (being defined by the number of data points), it provides a clear signature that long-term variations of the visual sporadic meteor rates are driven by the 11-year solar cycle.

## 4 Conclusions

In conclusion, we have investigated the activity of the sporadic meteors over a period of 26 years (1982–2007) on the basis of the available VMDB records. In the time interval of September 10–30, visual sporadic meteor hourly rates oscillate from year to year around the mean value of  $HR_{\text{spo}} = 11.7$  with an amplitude of  $\pm 20\%$  ( $\pm 2.3$ ). Statistical analysis reveals a certain periodicity of these oscillations, and the period (10.2 years) is almost coincides with 11-year solar activity cycle, represented by the Zurich sunspot numbers in this Paper.

These two processes exhibit a high degree of mutual correlation (0.36), indicating that the maximum visual sporadic meteor rates are recorded in the years of maximum sunspot numbers. Our result is much in contrast to that reported by Bumba (1949), who found exactly the opposite dependence (highest visual meteor rates occurring in the years of solar activity minimum). On the other hand, our findings for visual sporadic meteor rate variability are in good agreement with the results of the recent analysis of radar sporadic meteor rates carried out by Šimek and Pecina (2002). It has to be noted that the relationship of visual meteor rates in general and solar activity appears to be weaker in terms of the amplitude and maximum cross-correlation coefficient. These differences might be attributed to a different magnitude range of visual and radar meteors, and probably some smoothing effect which occurs due to time averaging of visual meteor counts.

Finally, in order to make our result more conclusive, it is necessary to investigate variations of visual sporadic meteor rates at other times of the year, and/or extend, if available, the analysis over a longer range of years.

## References

- Arlt R. (2003). "Bulletin 19 of the International Leonid Watch: population index study of the 2002 Leonid meteors". *WGN*, **31:3**, 77–87.
- Arlt R. and Rendtel J. (2006). "A new working list of meteor showers". *WGN*, **34:3**, 77–84.
- Bumba V. (1949). "Influence de l'activité solaire sur le nombre des observations de météores, de traînées météoriques et de chutes météoritiques". *Bull. Astron. Inst. Czechosl.*, **1**, 93–95.
- DeLand M. T., Shettle E. P., Thomas G. E., and Olivero J. J. (2006). "A quarter-century of satellite polar mesospheric cloud observations". *J. Atmos. Solar Terr. Phys.*, **68**, 9–29.
- Ellyett C. D. and Kennewell J. A. (1980). "Radar meteor rates and atmospheric density changes". *Nature*, **287**, 521–522.
- Gadsden M. (1998). "The North-West Europe data on noctilucent clouds: a survey". *J. Atmos. Solar Terr. Phys.*, **60**, 1163–1174.
- Hughes D. W. (1974). "Meteor rates, volcanoes and solar cycle". *Nature*, **252**, 191–192.
- Hughes D. W. (1995). "Sir John F. Herschel, meteoroid streams and the solar cycle". *Vistas in Astronomy*, **39**, 335–346.
- Lean J. (1997). "The Sun's variable radiation and its relevance to Earth". *Ann. Rev. Astron. Astrophys.*, **35**, 33–67.
- Lean J. (2005). "Living with the variable sun". *Phys. Today*, **58:6**, 32–38.
- Lindblad B. A. (1976). "Meteor radar rates and the solar cycle". *Nature*, **259**, 99–101.
- Lindblad B. A. (1978). "Meteor radar rates, geomagnetic activity and solar wind vector structure". *Nature*, **273**, 732–734.
- Lindblad B. A. (2003). "Solar control of meteor radar rates". Technical Report ESA SP-535, 755–759 pages.
- Pecina P. and Šimek M. (1999). "Analysis of the Gem-inid meteor stream, 1958–1997, from radar observations". *Astron. Astrophys.*, **344**, 991–1000.
- Porubčan V. and Getman V. S. (1992). "Distribution of meteor heights and solar cycle activity". *Contrib. Astron. Skalnaté Pleso*, **22**, 33–39.
- Prikryl P. (2002). "Radar meteor rates and solar activity". *Bull. Astron. Inst. Czechosl.*, **34**, 44–50.
- Romejko V. A., Dalin P. A., and Pertsev N. N. (2003). "Forty years of noctilucent cloud observations near Moscow: database and simple statistics". *J. Geophys. Res.*, **108**, 8443.
- Šimek M. and Pecina P. (2002). "Radar sporadic meteor rates and solar activity". *Earth, Moon, Planets*, **88**, 115–122.